Article

Molecular Self-Assembly of Bile Acid-Phospholipids Controls the Delivery of Doxorubicin and Mice Survivability

Vedagopuram Sreekanth, Nihal Medatwal, Sanjay Pal, Sandeep Kumar, Sagar Sengupta, and Avinash Bajaj

Mol. Pharmaceutics, **Just Accepted Manuscript** • DOI: 10.1021/acs.molpharmaceut.7b00105 • Publication Date (Web): 30 Jun 2017

Molecular Self-Assembly of Bile Acid-Phospholipids Controls the Delivery of Doxorubicin and Mice Survivability

Vedagopuram Sreekanth,[1,2] Nihal Medatwal,[1,2] Sanjay Pal,[1,3] Sandeep Kumar,[1,2] Sagar Sengupta,[4] and Avinash Bajaj[1,*]

1: Laboratory of Nanotechnology and Chemical Biology, Regional Centre for Biotechnology, NCR Biotech Science Cluster, 3rd Milestone Faridabad-Gurgaon Expressway, Faridabad-121001, Haryana, India.

2: Manipal University, Manipal-576104, Karnataka, India.

3: KIIT University, Bhubaneswar-751024, Odisha, India.

4: National Institute of Immunology, Aruna Asaf Ali Marg, New Delhi-110067, India.

*Corresponding Author:

Email: bajaj@rcb.res.in

Ph: +91-124-2848831, Fax: +91-124-2848803

Abstract: Lipid composition in general determines the drug encapsulation efficacy and release kinetics from liposomes that impact the clinical outcomes of cancer therapy. We synthesized three bile acid phospholipids by conjugating the phosphocholine head group to the 3'-hydroxyl group of benzylated lithocholic acid (LCA), deoxycholic acid (DCA), and cholic acid (CA); and investigated the impact of membrane rigidity on drug encapsulation efficacy, drug release kinetics, anticancer effects, and mice survival. Liposomes with hydrodynamic diameter of 100-110 nm were subsequently developed using these phospholipids. Fluorescence-probe based quantification revealed more fluidic nature of DCA-PC- and CA-PC-derived liposomes, whereas the LCA-PC-derived are rigid in nature. Doxorubicin encapsulation studies showed ~75% encapsulation and ~38% entrapment efficacy of Doxorubicin using more fluidic DCA-PC, CA-PC derived liposomes as compared to ~58% encapsulation and ~18% entrapment efficacy in case of LCA-PC derived liposomes. *In vivo* anticancer studies in the murine model confirmed that Doxorubicin entrapped CA-PC liposomes compromise mice survival, whereas rigid drug entrapped LCA-PC-derived-liposomes increased mice survival with ~2-fold decrease in tumor volume. Pharmacokinetic and bio-distribution studies revealed ~1.5-fold increase in plasma drug concentration and ~4.0-fold rise in tumor accumulation of Doxorubicin on treatment with drug entrapped LCA-PC liposomes as compared to Doxorubicin alone. In summary, this study presents the impact of bile acid derived liposomes with different rigidity on drug delivery and mice survivability.

Keywords: Bile Acids, Phospholipids, Doxorubicin delivery, Molecular self-assembly

Introduction:

Efficient liposomal based drug delivery systems using different kinds of phospholipids has been commercialized for treatment of cancer and fungal infections.[1] The encapsulation of active drug ingredients either in the aqueous or lipid bilayer compartments form the premise of the strategy for liposomal formulations where drug entrapment efficacy and their release kinetics is contingent on the chemical nature and composition of lipid ingrediants.[2] Low drug encapsulation, poor retention efficiencies, instability of the liposomes and their uptake by the reticulo-endothelial system, non-specific leakage of the encapsulated drug, and poor accumulation at tumor sites are major limitations of the encapsulation strategy used for anticancer drug delivery.[3] Therefore, designing of phospholipids for drug delivery is an active area of research; and recent studies have stressed on fine-tuning of the physicochemical, mechanical, and structural properties of the lipids to control the release rates of encapsulated drugs.[4-7]

Numerous approaches using smart head group design,[8] interfacial chemical linkage in hydrophobic region,[9] or dimeric lipids[10] have been used to fine-tune the membrane properties of liposomes. Szoka *et al.* recently investigated the interactions of cholesterol-derived phospholipids with membranes and developed effective formulations for drug delivery.[11,12] Impermeable vesicles have been developed using confirmationally restricted phosphatidylethanolamine derivatives that provide rigidity and mechanical strength to vesicles.[13] Wang and co-workers showed superior stability and enhanced doxorubicin encapsulation using phospholipid vesicles reinforced with hydrogen bonding.[14] Phospholipids produced using thiol-yne chemistry were resistant to the action of phospholipases, thereby generating more stable vesicles.[15]

Chemical nature and composition of lipids affect the rigidity of liposomal membranes because the presence of double bonds render the membranes fluid, whereas steroidal lipids

rigidify the membranes.[16] Recent studies have shown that the composition of lipid membranes affects its fluidity, thereby regulating the release of the encapsulated drugs.[17] It has been shown that *in vivo* anticancer activity of the folate targeted Mitoxantrone encapsulated liposomes is contingent on lipid composition and fluidity of the membranes.[18] Zhu and coworkers studied the aggregation properties of PEGylated bile acids using lithocholic acid, deoxycholic acid, and cholic acid conjugated with different polyethyleneglycol chains; and their ability to encapsulate hydrophobic drugs.[19,20]

Earlier studies suggested that the inclusion of hydroxyl groups in the hydrophobic domains of lipids modulate the rigidity of the liposomes,[21] which might thereby regulate drug encapsulation efficacy and release kinetics from these liposomes (**Fig. 1**). Differential drug release kinetics from liposomes may impact anticancer treatment efficiency and survivability of tumor-bearing mice. Therefore, we synthesized three bile acid-phosphocholine (BPC)-derived phospholipids using lithocholic acid (LCA), deoxycholic acid (DCA), and cholic acid (CA), namely, **LCA-PC**, **DCA-PC**, and **CA-PC,** which differ in the number of hydroxyl groups on their backbone (**Fig. 1**). These phospholipids were subsequently used to form liposomes for encapsulation of Doxorubicin, a model anticancer drug. Studies on anticancer activity and survival in a murine tumor model, along with pharmacokinetic and bio-distribution studies of the liposomes were performed to determine the impact of rigidity and drug release kinetics on tumor regression and mice survivability. This study will provide new insights on impact of membrane rigidity using bile acid derived phospholipids on doxorubicin delivery.

Experimental Section:

Materials and Methods: All solvents and chemicals used are of ACS grade. Lithocholic acid (LCA), deoxycholic acid (DCA), cholic acid (CA), benzyl bromide, L-α-Phosphatidylcholine (EggPC), 2-chloro-1,3,2-dioxaphospholane-2-oxide, Doxorubicin.HCl,

and Diphenylhexatriene (DPH) was purchased from Sigma-Aldrich. 1,2-distearoyl-sn-glycero-3-phosphoethanolamine-N-[amino(polyethyleneglycol)-2000] ammonium salt (DSPE-PEG2000-Amine) was purchased from Avanti-polar lipids. Unless mentioned, all compounds were purified using Combi-flash chromatography (Teledyne ISCO) using silica gel redi-sep or C_{18} silica redi-sep columns. NMR spectra were recorded on Brucker-Avance-400 MHz FT-NMR spectrometer. Chemical shifts are reported in δ ppm with reference to respective deuterated solvent. Mass spectra were recorded with AB SCIEX Triple TOF 5600 system. Synthesis and characterization of bile acid-phosphocholine (BPC)-derived phospholipids is reported in supporting information.

Determination of critical miceller concentration:[22] Stock solutions of LCA-PC, DCA-PC and CA-PC were prepared in ethanol; and serial dilutions were done in ethanol at 4 °C. Ethanol from the samples was evaporated in speed-vac for 1 hour at 37 °C. Samples were then suspended in 1 mL of pyrene solution (1.0 μg/mL), followed by vortexing, and fluorescence was recorded at 375 and 395 nm with excitation of 334 nm. Fluorescence ratio (395 nm/375 nm) was plotted against the concentration of compounds.

Liposome preparation and doxorubicin encapsulation: Doxorubicin.HCl was encapsulated in liposomes using remote drug loading method.[23] Typically Egg PC (5 mg), BPC (5 mg), and DSPE-PEG2000-Amine (1 mg) were taken in chloroform (0.2 mL) in 1: 1: 0.2 weight ratio in a round bottom flask. Chloroform is evaporated by rotary evaporation followed by vacuum pump to form a dry thin film. Thin films were hydrated with 250 mM ammonium sulfate solution (2 mL) at 60 ˚C for two hours with intermittent sonication at 60 ˚C for 1 min at 15 minutes interval. Lipid suspension was sequentially extruded through 200 (14 times) and 100 nm polycarbonate (14 times) membranes at 60 ˚C. Free ammonium sulfate was removed by dialysis (Spectrapor/CE, molecular weight cut off 100 KD, Spectrum laboratories Inc. USA.) of liposomes against 25 volumes of 5% glucose for 4

times in 24h. Liposomes were then incubated with Doxorubicin.HCl (5mg) in 5% glucose (1 mL) at 60 ˚C. Liposomal suspension was cooled down to room temperature, and mixed with activated Dowex 50WX-4 200 ion exchange to remove free or surface bound doxorubicin, rotated for 20 minutes, and filtered to get doxorubicin encapsulated liposomes. All these experiments were performed at least three times.

Encapsulation and entrapment efficiency: Encapsulation efficiency (concentration of drug present in liposomes) was determined using absorbance method[24] where liposomes (10 µL) were treated with 90% isopropyl alcohol containing 0.075 N HCl (190 µL), followed by measurement of Doxorubicin absorbance at 480 nm. Percentage of encapsulated Doxorubicin content was calculated by formula (I)

Encapsulation efficiency (% Doxorubicin encapsulated) = $(A_d/A_i) \times 100$……(I)

where A_i = initial absorbance of the sample where 5 mg of Doxorubicin was added.

A_d = final absorbance after Dowex treatment.

To determine the entrapment efficiency (drug to lipid weight ratio), we calculated the amount of phospholipids retained after extrusion of liposomes by colorimetric method.[25] Different linear concentrations of phospholipids and sample (10 µL) were diluted with chloroform (2 mL) and then treated with 1 mL ferrothiocyante reagent. Samples were vortexed for 20 sec. and spun for 10 min at 1000 *r.p.m* to remove out the lower layer. Absorbance of standards and samples was read at 488 nm; and concentration of phospholipids present in the test sample was computed using standard curve. Percentage of phospholipid content retained was plotted using following formula (II)

% Phospholipids retained = $[PL]_d/[PL]_i \times 100$ ……(II)

whereas $[PL]_i$ = concentration of total phospholipids used for liposome preparation before extrusion.

$[PL]_d$ = concentration of phospholipids retained after extrusion

Entrapment efficiency was calculated using following formula (III)

Entrapment efficiency (%) = $[Dox]_d$ /$[PL]_d$ × 100 ……...(III)

$[DOX]_d$ = Doxorubicin concentration after dowex treatment.

$[PL]_d$ = Phospholipid concentration in liposomes after extrusion.

In vitro **drug release experiments:** *In vitro* drug release experiments were conducted using dialysis method in three different conditions.[26] Typically doxorubicin encapsulated liposomes (1 mL) were placed in dialysis tubing (Spectrapor/CE, molecular weight cut off 100 KD, Spectrum laboratories Inc. USA.) and dialyzed against 30 mL of different release buffer conditions (pH 7.4, PBS; pH 5.0, PBS; 10% FBS in PBS) at 37 ˚C away from bright light. At various time points; aliquots (1 mL) were withdrawn from outer aqueous solution and replaced by fresh release medium (1 mL). Samples were stored at 4 ˚C until analysis were performed spectrofluorimetrically using Molecular devices M5 instrument with λ_{ex} of 480 nm and λ_{em} of 590 nm. Rate and percentage of drug released was computed using following formula (IV)

Percentage of drug released = $[Dox]_t/[Dox]_i$ × 100 …….(IV)

where $[Dox]_t$ = Doxorubicin concentration released at time t.

$[Dox]_i$ = Doxorubicin concentration in doxorubicin entrapped liposomes in dialysis tube.

We then computed release rate constants using Higuchi model[27] by fitting release data in following equation (V)

Amount of doxorubicin released at time t

$[Dox]_t = K_H \times (t)^{1/2}$ …….(V)

where K_H = Higuchi rate constant.

t = corresponding time t.

Dynamic light scattering and zeta potential: Mean particle size (*Z*-avg. diameter), polydispersity index (pdI), and zeta potential of liposomes were measured by Dynamic Light Scattering method using Zetasizer NanoZS90 (Malvern, UK). Liposomal suspension (100 µL) was diluted to 1 mL using PBS and 3 sets of 11 measurements were performed at 90˚ scattering angle to get average particle size and pdI for each liposome. Zeta potential of liposomes was measured using zeta cuvette at 173˚ scattering angle.

Transmission electron microscopy: For negative stain transmission electron microscopy (TEM), bile acid suspension (~5 mM) was deposited on to a sample grid. Samples were then stained with 1% phosphotungstic acid for 10 minutes and dried with whatman filter paper. Samples were observed under FEI Tecnai TF20 transmission electron microscope, and images were processed using Tecnai G2 software.

Membrane rigidity studies: Hydrated thin films of EggPC, BPC, and DSPE-PEG2000-Amine (1:1:0.2 weight ratio) (as prepared above) were processed for 4-5 freeze thaw cycles from 70 ˚C to 4 ˚C with intermittent vortexing followed by sonication at 70 ˚C for 15 min. For anisotropy studies, 1% Diphenyl hexatriene (DPH) was incorporated during thin film preparation.[21] Steady state DPH anisotropy measurements were carried out at 37 ˚C in 96-well plate and anisotropy was calculated as per published protocol.[21]

Cell culture: Murine (4T1) and human (MDA-MB-231) breast cancer cells were maintained as monolayers in RPMI-1640 (for 4T1 cells) or DMEM (Hyclone, USA) (for MDA-MB-231 cells) media containing 10% (v/v) fetal bovine serum, penicillin (100 µg/mL), streptomycin (100 U/mL), and gentamycin (45 µg/mL) at 37 ˚C in a humidified atmosphere with 5% CO_2; and subcultures were made by trypsinization.

MTT assay: Cytotoxicity of bile acids, doxorubicin, BPCs, and doxorubicin entrapped BPC liposomes was estimated using MTT {3-(4, 5-dimethylthiazol-2-yl)-2, 5-diphenyltetrazolium bromide} assay. MTT was dissolved in PBS at a concentration of 5 mg/mL and filtered.

Approximately ~3000 cells/well were seeded in 96 well plates containing 200 µL of complete medium. After 24h of pre-culture period to ensure cell attachment, medium was replaced with fresh medium supplemented with different concentrations of BPCs, doxorubicin, or doxorubicin entrapped liposomes. After 48 h of treatment, 20 µL of MTT solution was added to each well and incubated for 4 h. Formazan crystals formed were then dissolved in 1:1 mixture of DMSO and methanol and optical density (OD) of each well was measured using a micro culture plate reader at 540 nm. Percentage viability was then calculated as [{A540 (treated cells) - background]/[A540 (untreated cells) - background}] x 100.

***In vivo* anticancer and toxicological studies:**[28] All animal experiments were done with approval of Institutional Animal Ethical Committee (IAEC), National Institute of Immunology, New Delhi. Murine breast cancer (4T1) cells (1.5×10^6) in 200 µL FBS were injected subcutaneously into right flanks of 5-week-old female Balb/c mice. Mice were randomized into six groups (9 mice in each group) after they develop tumor of ~75 mm^3. Groups were then subjected to different treatments of a) 5% glucose (control group); b) free doxorubicin; and doxorubicin encapsulated c) LCA-PC liposomes, d) DCA-PC liposomes, e) CA-PC liposomes, f) Adrisome^{TM} (Positive control) with an equivalent doxorubicin dose of 5 mg/kg, intravenously through lateral tail vein on alternate day (total three doses). Tumor measurements were made every alternate day using digital caliper, and tumor volume was calculated using formula $L \times B^2/2$ where L and B are length and breadth of tumor. Survival study was continued till the last mouse was found live in all the groups. To test the effect of neat liposomes without doxorubicin, 4T1-tumor bearing mice were randomized into four groups a) untreated, b) LCA-PC, c) DCA-PC, and d) CA-PC liposomes treated group, where mice were treated with three doses of 20 mg/kg (phospholipid content) of liposomes on alternate day; and tumor volumes and body weights were measured on alternate days.

For toxicological studies, two groups (n = 3) of tumor (4T1) bearing mice (200 mm^3) were administered with a single intravenous dose (equivalent to 5 mg/kg of doxorubicin) of free doxorubicin and doxorubicin entrapped LCA-PC liposomes respectively. Bleeds were taken post 24 h treatment and plasma/serum samples were processed for estimation of cardiac muscle specific toxicity marker (CK-MB), muscular toxicity marker lactate dehydrogenase (LDH), and liver specific toxicity marker alkaline phosphatase (ALP). Estimations were carried out at certified Newmax care pathological laboratory at New Delhi.

Pharmacokinetics and bio-distribution studies: Tumor (4T1) bearing mice (200 mm^3) were randomized into three groups a) control group (n= 3 mice), b) doxorubicin treated group (n = 3 per time point), c) doxorubicin entrapped LCA-PC liposomes treated group (n = 3 per time point). Mice in group b and c were administered with a single intravenous dose (equivalent to 5 mg/kg of doxorubicin) of free doxorubicin and doxorubicin entrapped LCA-PC liposomes respectively. Serial bleeds were collected in ACD-micro centrifuge tube through orbital sinus under mild ketamine-xylazine anesthesia at 0.08, 0.25, 0.5, 1, 5, 10, and 24 h after intravenous injection. Plasma was separated from samples and stored under -80 ˚C until analysis. At time points of 1, 5, and 10 h; mice were sacrificed; and tumor, liver, spleen, kidneys, lungs, and heart were removed after blood withdrawal, washed with ice cold PBS, weighed, and stored in -80 ˚C until analysis.

We extracted drug content present in 100 µL of plasma and 100 mg of respective tissue samples using 500 µL acidified alcohol (90% isopropanol with 0.75 N HCl). Tissue samples with extracting solvent were placed in 2 mL homogenization tubes and homogenized with zirconia beads by bead beating at 5000 rpm. Plasma samples were transferred to 2 mL tubes and mixed with 500 µL of acidified alcohol. Homogenized tissue samples and plasma samples were stored in 4 ˚C overnight to extract the drug. Samples were then centrifuged at 14,000 rpm for 5 min at 4 ˚C. Supernatant liquid was transferred to fresh tube and solvent

was completely evaporated using speed-vac. Final residue was dissolved in 200 µL acidified alcohol and transferred to 96-well plates. Analysis was performed spectrofluorimetrically using Molecular devices M5 instrument with λ_{ex} of 480 nm; and λ_{em} of 590 nm. A calibration curve was prepared for doxorubicin using concentrations from 5-5000 ng/mL in acidified alcohol. Final fluorescence values were obtained by subtracting background fluorescence from each tissue type. A graph was plotted against concentration of doxorubicin versus different time points for pharmacokinetics and concentration of doxorubicin versus each tissue type at different time points for bio-distribution studies. Plasma drug concentration data was fitted and pharmacokinetic analysis were performed using WinNonLin (Version 6.4).[29]

Results and Discussion:

Design and synthesis of bile acid-phospholipids: Bile acids are interesting scaffolds for biomaterials as their biocompatible nature and adaptability for bioconjugation chemistry can be applied in biomedicine[30] for drug delivery,[31] as potential inhibitors,[32] antimicrobial agents,[33] siRNA delivery,[34] as hydrogels,[35] and sensors.[36] Natural bile acids differ from each other in the number and stereochemistry of free hydroxyl groups present on the concave side of the hydrophobic backbone.[37] The membrane properties of liposomes depend on the amphiphilic nature of bile acids and their unique structural features that can impact the biomedical applications.[38] Therefore, we synthesized bile acids with varying number of hydroxyl groups for liposome preparation and explored their use for drug delivery.

We selected three bile acids—LCA, DCA, and CA—and designed three bile acid-phosphocholine (BPC)-derived phospholipids, where the phosphocholine head group was appended to the 3'-hydroxyl group of bile acids (**Fig. 1**). The C_{24}-carboxyl group of bile acids **(4-6)** was initially protected by benzyl esters[39] **(7-9)** that were reacted with 2-chloro-1,3,2-

dioxaphospholane-2-oxide to produce unstable intermediates **(10-12)** and a triethylamine hydrochloride (NEt_3.HCl) salt (**Scheme 1**). The reaction mixture was filtered through celite and immediately reacted with trimethylamine in an Ace pressure tube to generate phospholipid conjugates **(1-3)**.[40] Purification of these conjugates by reverse phase C_{18} silica combiflash column chromatography yielded 60-65% of the final phospholipids **(1-3)** (**Scheme1**), which were characterized by ^{1}H-NMR, ^{13}C-NMR, ^{31}P-NMR, and HRMS (Supporting information).

Liposome preparation and characterization: We first, determined the critical miceller concentration (CMC) of the LCA-PC, DCA-PC and CA-PC using Pyrene-Fluorescence based method.[22] CMC of LCA-PC, DCA-PC and CA-PC were found to be 12, 22 and 51 μM (**Figure S1**) suggesting that increase in number of hydroxyl groups enhances the CMC as reported in earlier studies as well.[41] We then tested the ability of BPCs to form self-assembled aggregates without addition of any helper lipid. Transmission electron microscopy (TEM) of the negative-stained aggregates revealed their spherical nature of 90-120 nm, where the LCA-PC aggregates were smaller in size than the formed by DCA-PC and CA-PC (**Fig. 2A-2C**). Next, we used a mixture of BPC, EggPC, and DSPE-PEG 2000-amine in a weight ratio of 1:1:0.2 to form liposomes, where the Egg PC and DSPE-PEG 2000-amine promoted efficient encapsulation[42] and stealthing of liposomes[43], respectively. Hydrated films of the lipid mixture were then subjected to 14 cycles of extrusion to obtain desired liposomes. Quantification of phospholipid content analysis showed an average 73, 47, and 44 % retention of phospholipids after extrusion in case of LCA-PC, DCA-PC and CA-PC liposomes respectively. Dynamic light scattering (DLS) studies showed a monomodal size distribution of 100-110 nm (**Fig. 2D-2G**) with a polydispersity index of 0.1-0.2 (**Fig. 2H**) and zeta potential ranging from 12-22 mV (**Fig. 2I**).

Drug encapsulation efficacy: Next, we tested the doxorubicin (a model water soluble

anticancer drug) encapsulation ability of BPC liposomes using a remote drug loading method,[23] and observed ~58% drug encapsulation for LCA-PC and ~75% drug encapsulation for both DCA-PC and CA-PC liposomes (**Fig. 3A**). The presence of free hydroxyl groups increased the fluidity of DCA-PC and CA-PC liposomes, which allowed them to entrap additional doxorubicin molecules in the lipid bilayer than the non-hydroxylated LCA-PC liposomes. Estimation of the phospholipids retained by liposomes revealed that LCA-PC liposomes had higher lipid content (73%) than DCA-PC and CA-PC liposomes (~40%) because of better packing of LCA-PC in the membranes (**Fig. 3B**). Therefore, the entrapment efficiency of DCA-PC and CA-PC liposomes was around 38%, whereas it was ~18% for LCA-PC liposomes (**Fig. 3C**).

Drug release kinetics: We investigated the release kinetics of doxorubicin from BPC liposomes under the following conditions: (a) physiological pH using phosphate buffer saline (PBS, pH 7.4), (b) acidic tumor microenvironment (acetate buffer, pH 5.0), and (c) blood serum (10% fetal bovine serum (FBS) in PBS, pH 7.4) at 37 ^{o}C (**Fig. 3D-3F; Fig. S2**). The initial burst release of doxorubicin was observed from all the three liposomes at pH 7.4, and the cumulative doxorubicin release was below 50%. Although we observed a slight increased rate of doxorubicin release at both pH 7.4 and pH 5.0, there were no distinct differences in drug release among the three liposomes. Marked differences in the rates of doxorubicin release in FBS were observed among these liposomes as serum proteins are known to interact with liposomes and cause burst release of the encapsulated contents.[44] We observed faster release rate and enhanced doxorubicin release content (~80%) from the hydroxylated DCA-PC and CA-PC liposomes, whereas the LCA-PC liposomes maintained a sustained release of doxorubicin with a maximum ~60% release of contents. The Higuchi release rate constants[45] with R^2 > 90% confirmed the differential drug release kinetics of BPC liposomes in blood serum conditions, and LCA-PC liposomes showed the

slowest release of doxorubicin (**Fig. 3G**). We believe that the differential drug release patterns of BPC liposomes might arise from the distinct packing of phospholipids in the lipidated liposomes, which allows faster release of the loosely encapsulated doxorubicin from DCA-PC and CA-PC liposomes. Therefore, we probed the effect of BPCs on membrane fluidity using diphenylhexatriene (DPH)-based membrane probe.

Membrane rigidity studies: The anisotropy of DPH, a rigid fluorophore, is reduced when it transits from a tightly packed environment to fluidic conditions as perturbations in the internal packing of membranes allow random movement of DPH.[21] Anisotropy studies revealed marked differences in the rigidity of hydroxylated and non-hydroxylated phospholipid liposomes (**Fig. 3H**). Membranes containing LCA-PC were highly rigid due to better packing efficiency of LCA-PC lipids in membranes, whereas membranes containing DCA-PC and CA-PC were comparatively fluid in nature. Rigid packing of LCA-PC causes slow release of doxorubicin, whereas the fluidic nature of hydroxylated phospholipids (DCA-PC and CA-PC) induces enhanced encapsulation with faster drug release kinetics (**Fig. 3H**). Therefore, distinct differences in membrane rigidity of lipidated liposomes that vary in number of free hydroxyl groups are responsible for marked differences in encapsulation and drug release from BPC liposomes.

***In vitro* cytotoxicity studies:** We first tested the cytotoxicity of phospholipids and compared with corresponding bile acids against murine (4T1) and human (MDA-MB-231) breast cancer cell lines (**Fig. S3**, **Table S1**). Among bile acids, LCA, DCA and CA; hydrophilic CA is non-toxic to both the cells at concentrations tested whereas hydrophobic LCA has IC_{50} of ~182 and 309 μM against 4T1 and MDA-MB-231 cells respectively. DCA in contrast was non-toxic to MDA-MB-231 cells but has IC_{50} of ~261 μM against murine cell lines. Phosphatidylcholine conjugation to bile acids make them more toxic for both the cells where LCA-PC and DCA-PC has IC_{50} of ~73 and ~150 μM against 4T1 and MDA-MB-231

cells respectively; whereas CA-PC was toxic only to murine cancer cells. The toxic concentrations of bile acid phospholipids are much higher than the concentrations used for doxorubicin delivery.

Anticancer activities of doxorubicin-encapsulated BPC liposomes were then studied in murine (4T1) and human (MDA-MB-231) breast cancer cell lines. Interestingly, we observed that human MDA-MB-231 cells were less susceptible to liposomal formulation as compared to murine 4T1 breast cancer cells (**Fig. 4, S3**). As expected 48h exposure was more toxic to the cells as compared to 24h exposure. After 24h of exposure to 4T1 murine cancer cells, drug entrapped CA-PC liposomes were more toxic as compared to drug encapsulated LCA-PC liposomal formulations due to fast drug release from drug-entrapped CA-PC liposomes. All drug-entrapped BPC liposomal formulations in general were found to induce cell death in both the cell lines after 48 h, indicating effective release of doxorubicin from the liposomes (**Fig. 4**).

***In vivo* antitumor activities:** We first tested the effect of neat LCA-PC, DCA-PC and CA-PC liposomes without Doxorubicin encapsulation on tumor regression, where mice were treated with three doses of liposomes. As shown in **Fig. S4**, none of the liposomal formulation induce any effect of tumor proliferation thereby concluding that these liposomal formulations are safe and does not induce any cytotoxicity,

The frequency of chemotherapy schedules depends on the elicited toxicity, tumor regression, and survival response of the patients. Frequent chemotherapeutic schedules enhance tumor regression, albeit with high toxicity and poor survival. Therefore, to understand the impact of BPC liposomes on anticancer activity, toxicity, and survival, we evaluated the potency of doxorubicin encapsulated BPC liposomes against 4T1 murine breast cancer model in Balb/c mice. Tumor-bearing animals were randomized into six groups of nine animals each when the average tumor size reached a volume of ~75 mm^3;

the animals were administered with (a) 5% glucose (control group), (b) free doxorubicin, and doxorubicin entrapped in (c) LCA-PC, (d) DCA-PC, (e) CA-PC; and f) Adrisome^{TM} liposomes at an equivalent doxorubicin dose of 5 mg/kg for three alternate days. We observed a ~40-50% reduction in tumor volume upon treatment with doxorubicin loaded BPC liposomes as compared to untreated control whereas Adrisome^{TM} treated mice did not show any progression of tumor growth (**Fig 5A**). Drug release from the liposomal formulations impacts the tumor regression, toxicity, and survival of the mice as tumor regression with enhanced toxicity of poor survival is not recommended. We therefore, compared the mice survivability of tumor bearing mice on different treatments. Mice treated with doxorubicin alone without any carrier could not enhance the mice survivability due to its toxic nature. We observed a differential impact on mice survival on treatment with drug encapsulated liposomes irrespective of the differences in body weights of the drug-treated mice (**Fig 5B**). Mice treated with LCA-PC liposomes showed significant improvement in survival than that observed with DCA-PC and CA-PC liposomes (**Fig. 5C**) whereas mice treated with drug-loaded CA-PC liposomes died before the untreated tumor-bearing mice in spite of 50% tumor regression due to the high toxicity of the free drug present in the blood circulation. We observed the similar effect during *in vitro* studies where doxorubicin-entrapped CA-PC liposomes are more toxic to murine cancer cells as compared to drug-entrapped LCA-PC liposomes. Therefore, rigid LCA-PC liposomes triggered a significant increase in mice survival compared to the poor survival rate of the DCA-PC- and CA-PC-liposomes treated mice. The un-entrapped doxorubicin treated mice showed sudden weight loss and decline in survival.

To investigate this, we estimated and compared the levels of lactate dehydrogenase (LDH; muscle tissue marker), cardiac muscle-specific creatinine phosphokinase (CK-MB), and alkaline phosphatase (ALP for liver toxicity) in mice serum after 24 h of treatment with free

doxorubicin and doxorubicin-entrapped LCA-PC liposomes. We observed a significant decrease in ALP levels **(Fig. 5D);** and an increase in circulatory levels of LDH **(Fig. 5E)** and CK-MB **(Fig. 5F)** upon doxorubicin treatment, whereas the doxorubicin-entrapped LCA-PC liposomes did not elicit any toxic response in the tumor-bearing mice. Higher circulatory levels of these markers in mice treated with free doxorubicin could possibly explain the cardiac toxicity and loss in muscle mass of these animals.

Pharmacokinetics and bio-distribution studies: To estimate the doxorubicin concentration in plasma and other body organs, we performed pharmacokinetic and bio-distribution studies in 4T1 tumor bearing Balb/c mice that were randomized into three groups: (a) untreated control (n = 3), (b) free doxorubicin (n = 3 per time point), and (c) doxorubicin-entrapped LCA-PC liposomes (n = 3 per time point). Mice in groups (b) and (c) were treated with equivalent doses of doxorubicin (5 mg/kg) and pharmacokinetic parameters were estimated by the two-compartment single intravenous bolus model. We observed ~1.5-fold increase in plasma concentration of Doxorubicin on treatment with drug entrapped LCA-PC liposomes as compared to doxorubicin alone (**Fig. 5G, 5H**) with similar mean resident time (MRT) for LCA-PC liposomes and doxorubicin. There was ~1.5-fold increase in drug availability using doxorubicin entrapped liposomes as compared to doxorubicin alone (**Fig. 5H**).

Bio-distribution studies revealed a three-fold increase in doxorubicin concentration at the tumor site upon treatment with LCA-PC liposomes than that observed with doxorubicin alone (**Fig. 5I-5K**). We observed negligible doxorubicin concentration in vital organs such as the heart and lungs. Treatment with doxorubicin-entrapped LCA-PC liposomes lowered the accumulation of doxorubicin in the kidneys, implying enhanced blood circulation compared to that observed upon treatment with free doxorubicin (**Fig. 5I-5K**).

Conclusions: In summary, we developed three bile acid-phosphocholine-derived phospholipids that differ in the number of free hydroxyl groups. Drug encapsulation and release studies revealed that increased fluidity of membranes enhanced drug encapsulation efficacy of liposomes. The highly fluid liposomes allowed burst release of drugs, whereas the rigid liposomes maintained a sustained release of drugs. *In vivo* studies in murine models confirmed that survival of tumor-bearing mice is contingent on the drug release kinetics, where the hydrophobic liposomes caused tumor regression with increased survival rates. Therefore, this study provides new insights into designing of bile acid-derived lipidated liposomes, which will assist in the development of future cancer therapies.

Acknowledgements: We thank RCB and NII for intramural funding, and Department of Biotechnology (DBT) for supporting this project. VS, NM, SP, and SK thank RCB, UGC and CSIR for research fellowship. We thank Dr. Aniruddha Sengupta and Mr. Mallik Samarla for helping us in analyzing pharmacokinetic data.

Author contributions: AB conceived idea. VS and AB designed the experiments. VS synthesized molecules. VS and NM carried out liposomal drug encapsulation and release studies. SP and VS carried out *in vivo* studies. SK performed biophysical studies. SS supervised the animal studies. VS and AB wrote manuscript.

Supporting information: Synthesis of Bile acid-phospholipids, cytotoxicity of bile acids and Bile acid-Phospholipids, CMC of amphiphiles, Drug release studies till 48h, ^{1}H-NMR, ^{13}C-NMR, ^{31}P-NMR and HRMS of final compounds is available in supporting information.

References:

1) Torchillin, V. P. Recent advances with liposomes as pharmaceutical carriers. *Nat. Rev. Drug. Discov*. **2005,** *4*, 145-160.

2) Chang, H.; Yeh, M. Clinical development of liposome-based drugs: formulation, characterization, and therapeutic efficacy. *Int. J. Nanomed.* **2012**, *7*, 49–60.

3) Sharma, A.; Sharma, U. S. Liposomes in drug delivery: Progress and limitations. *Int. J. Pharm.* **1997,** *154*, 123-140.

4) Alavizadeh, S. H.; Badiee, A., Golmohammadzadeh, S.; Jaafari, M. R. The influence of phospholipid on the physicochemical properties and anti-tumor efficacy of liposomes encapsulating cisplatin in mice bearing C26 colon carcinoma. *Int. J. Pharm.* **2014**, *473*, 326-333.

5) Oussoren, C.; Eling, W. M.; Crommelin, D. J.; Storm, G.; Zuidema, J. The influence of the route of administration and liposome composition on the potential of liposomes to protect tissue against local toxicity of two antitumor drugs. *Biochim. Biophys. Acta.* **1998,** *1369*, 159-172

6) Mayer, L. D.; Tai, L. C.; Ko, D. S.; Masin, D.; Ginsberg, R. S.; Cullis, P. R.; Bally, M. B. Influence of vesicle size, lipid composition, and drug-to-lipid ratio on the biological activity of liposomal doxorubicin in mice. *Cancer Res.* **1989**, *49*, 5922-5930.

7) Johnston, M. J.; Edwards, K.; Karlsson, G.; Cullis, P. R. Influence of drug-to-lipid ratio on drug release properties and liposome integrity in liposomal doxorubicin formulations. *J. Liposome Res.* **2008**, *18*, 145-157.

8) Bhargava, P.; Singh, M.; Sreekanth, V.; Bajaj, A. Nature of the charged headgroup determines the fusogenic potential and membrane properties of lithocholic acid phospholipids *J. Phys. Chem. B* **2014**, *118*, 9341–9348.

9) Bhattacharya, S.; Dileep, P.V. Membrane-forming properties of cationic lipids bearing oxyethylene-based linkages. *J. Phys. Chem. B*, **2003**, *107*, 3719–3725

10) Kumar, S.; Bhargava, P.; Sreekanth, V.; Bajaj, A. Design, synthesis, and physico-chemical interactions of bile acid derived dimeric phospholipid amphiphiles with model membranes. *J. Colloid Interface. Sci.* **2015**, *448*, 398-406.

11) Huang, Z.; Szoka, Jr. F. C. Sterol-modified phospholipids: Cholesterol and phospholipid chimeras with improved biomembrane properties. *J. Am. Chem. Soc.* **2008**, *130*, 15702–15712.

12) Huang, Z.; Jaffari, M. R.; Szoka, Jr. F. C. Disterolphospholipids: nonexchangeable lipids and their application to liposomal drug delivery. *Angew. Chem. Int. Ed.* **2009**, *48*, 4146–4149.

13) Vares, L.; Koulov, A. V.; Smith, B. D. Highly impermeable vesicles composed of conformationally restricted phosphatidylethanolamine. *Chem. Commun*. **2002**, *14*, 1482-1483.

14) Wang, D.; Tu, C.; Su, Y.; Zhang, C.; Greiser, U.; Zhu, X.; Yana, D.; Wang, W. Supramolecularly engineered phospholipids constructed by nucleobase molecular recognition: upgraded generation of phospholipids for drug delivery. *Chem. Sci.* **2015**, *6*, 3775-3787.

15) Zhou, C. Y.; Wua, H.; Devaraj, N. K. Rapid access to phospholipid analogs using thiol-yne chemistry. *Chem. Sci.* **2015**, *6*, 4365–4372.

16) Bhattacharya, S.; Biswas, J. Understanding membranes through the molecular design of lipids. *Langmuir*, **2010**, *26*, 4642-4654.

17) Shimanouchi, T.; Ishii, H.; Yoshimoto, N.; Umakoshi, H.; Kuboi, R. Calcein permeation across phosphatidylcholine bilayer membrane: Effects of membrane fluidity, liposome size, and immobilization. *Colloids Surf. B Biointerfaces*. **2009**, *73*, 156-160.

18) Kawano, K.; Onose, E.; Hattori, Y.; Maitani, Y. Higher liposomal membrane fluidity enhances the in vitro antitumor activity of folate-targeted liposomal mitoxantrone. *Mol Pharm.* **2009**, *6*, 98-104.

19) Dévédec, F. L.; Fuentealba, D.; Strandman, S.; Bohne, C.; Zhu, X. X. Aggregation behavior of pegylated bile acid derivatives. *Langmuir*, **2012**, *28*, 13431-13440.

20) Dévédec, F. L.; Strandman, S.; Hildgen, P.; Leclair, G.; Zhu, X. X. PEGylated bile acids for use in drug delivery systems: enhanced solubility and bioavailability of Itraconazole. *Mol. Pharm.* **2013**, *10*, 3057-3066.

21) Sreekanth, V.; Bajaj, A. Number of free hydroxyl groups on bile acid phospholipids determines the fluidity and hydration of model membranes. *J. Phys. Chem. B* **2013**, *117*, 12135-12144.

22) Basu Ray, G.; Chakraborty, I.; Moulik, S. P.; Pyrene absorption can be convenient method for probing critical miceller concentration (cmc) and indexing miceller polarity, *J. Colloid Interface Sci.* **2006**, *294*, 248-254.

23) Bolotin, E. M.; Cohen, R.; Bar, L. K.; Emanuel, N.; Ninio, S.; Lasic, D. D.; Barenholz, Y. Ammonium sulfate gradients for efficient and stable remote loading of amphipathic weak bases into liposomes and ligandoliposomes. *J. Liposome Res.* **1994**, *4*, 455-479.

24) Amselem, S.; Cohen, R.; Druckmann, S.; Gabizon, A.; Goren, D.; Abra, R. M.; Huang, A.; New, R.; Barenholz, Y. Preparation and characterization of liposomal doxorubicin for human use. *J. Liposome Res.* **1992**, *2*, 93-123.

25) Sterwart, J. C. M. Colorimetric determination of phospholipids with ammonium ferrothiocyanate. *Anal. Biochem.* **1980**, *104*, 10-14.

26) Hua, S. Comparison of *in vitro* dialysis release methods of loperamide encapsulated liposomal gel for topical drug delivery. *Int. J. Nanomedicine.* **2014**, *9*, 735-744.

27) Siepmanna, J.; Peppas, N. A. Higuchi equation: derivation, applications, use and misuse. *Int. J. Pharm.* **2011**, *418*, 6-12.

28) Sengupta, P.; Basu, S.; Soni, S.; Pandey, A.; Roy, B.; Oh, M. S.; Chin, K. T.; Paraskar, A. S.; Sarangi, S.; Connor, Y.; Sabbisetti, V. S.; Kopparam, J.; Kulkarni, A.; Mutoc, K.; Amarasiriwardena, C.; Jayawardene, I.; Lupoli, N.; Dinulescu, D. M.; Bonventre, J. V.; Mashelkar, R. A.; Sengupta, S. Cholesterol-tethered platinum II-based supramolecular

nanoparticle increases antitumor efficacy and reduces nephrotoxicity. *Proc Natl Acad. Sci. USA* **2012**, *109*, 11294-11299.

29) Nders, C. K.; Adamo, B.; Karginova, O.; Deal, A. M.; Rawal, S.; Darr, D.; and Schorzman, A. Pharmacokinetics and efficacy of PEGylated liposomal doxorubicin in an intracranial model of breast cancer, *PLOS One*, **2013**, *8*, e61359.

30) Nonappa; Maitra, U. Unlocking the potential of bile acids in synthesis, supramolecular/materials chemistry and nanoscience. *Org. Biomol. Chem.* **2008**, *6*, 657-669.

31) Luo, J.; Xiao, K.; Li, Y.; Lee, J. S.; Shi, L.; Tan, Y. H.; Xing, L.; Cheng, H. R.; Liu, G. Y.; Lam, K. S. Well-defined, size-tunable, multifunctional micelles for efficient paclitaxel delivery for cancer treatment. *Bioconjugate Chem.* **2010**, *21*, 1216-1224.

32) Park, J.; Al-Hilal, T. A.; Jeong, J. H.; Choi, J. U.; Byun, Y. Design, synthesis, and therapeutic evaluation of Poly(acrylic acid)-tetraDOCA conjugate as bile acid transporter inhibitor. *Bioconjugate Chem.* **2015**, *26*, 1597-1605.

33) Lai, X.; Feng, Y.; Pollard, J.; Chin, J. N.; Rybak, M. J.; Bucki, R.; Epand, R. F.; Spand, R. M.; Savage, P. B. Ceragenins: Cholic acid-based mimics of antimicrobial peptides. *Acc. Chem. Res.* **2008**, *41*, 1233-1240.

34) Amjad, M. W.; Amin, M. C.; Katas, H.; Butt, A. M.; Kesharwani, P.; Iyer, A. K. *In Vivo* antitumor activity of folate-conjugated cholic acid-polyethylenimine micelles for the co-delivery of doxorubicin and siRNA to colorectal adenocarcinomas. *Mol. Pharm.* **2015**,*12*, 4247-4258.

35) Mukhopadhyay, S.; Maitra, U,; Krishnamoorthy, G.; Schmidt, J.; Talmon, Y. Structure ad dynamics of a molecular hydrogel derived from a tripodal cholamide, *J. Am. Chem. Soc.* **2004**, *126*, 15905-15914.

36) Khatri, V. K.; Chahar, M.; Pavani, K.; Pandey, P. S. Bile acid-based cyclic bisbenzimidazolium receptors for anion recognition: highly improved receptors for fluoride and chloride ions. *J. Org. Chem.*, **2007**, *72*, 10224-10226.

37) Mukhopadhyay, S.; Maitra, U. Chemistry and biology of bile acids, *Curr. Sci.* **2004**, *87*, 1666-1683.

38) Singh, M.; Singh, A.; Kundu, S.; Bansal, S.; Bajaj, A. Deciphering the role of charge, hydration, and hydrophobicity for cytotoxic activities and membrane interactions of bile acid based facial amphiphiles. *Biochim. Biophys. Acta* **2013**, *1828*, 1926-1937.

39) Qian, S.; Wu, J-B.; Wu, X-C.; Li, J.; Wu Y. Synthesis and characterization of new liver targeting 5-fluorouracil-cholic acid conjugates. *Arch. Pharm. Chem. Life, Sc*. **2009**, *342*, 513-520.

40) Sandbhor, M.S.; Key, J. A.; Strelkov, I. S.; Cairo, C. W. A Modular synthesis of alkynyl-phosphocholine head groups for labeling sphingomyelin and phosphatidylcholine. *J. Org. Chem.* **2009,** *74,* 8669-8674.

41) Monte, M. J.; Marin, J. JG.; Antelo, A.; Vazquez-tato, J. Bile acids: Chemistry, physiology, and pathophysiology, *World J. Gastroenterol.* **2009**, *15*, 804-816.

42) Harasym T. O.; Cullis, P. R; Bally, M. B. Intratumor distribution of doxorubicin following i.v. administration of drug encapsulated in egg phosphatidylcholine/cholesterol liposomes. *Cancer Chemother Pharmacol.* **1997**, 40, 309-317.

43) Palvai, S.; More, P.; Mapara, N.; Basu, S. Chimeric nanoparticle: A platform for simultaneous targeting of phosphatidylinositol-3-kinase signaling and damaging DNA in cancer cells, *ACS Appl. Mater. Interfaces*, **2015**, *7*, 18327-18335.

44) Agarwal, K.; Bali, A.; Gupta, C. M. Influence of the phospholipid structure on the stability of liposomes in serum. *Biochim. Biophys. Acta* **1986,** *856*, 36-40.

45) Paul, D. R. Elaborations on the Higuchi model for drug delivery. *Int. J. Pharm.* **2001**, *418*, 13-17.

Figure Legends

Figure 1. Design of BPCs: Molecular structures and schematic presentation of Lithocholic Acid (LCA), Deoxycholic Acid (DCA), and Cholic Acid (CA) derived phospholipids **LCA-PC**, **DCA-PC** and **CA-PC**; and schematic representation depicting the impact of membrane packing on encapsulation efficacy and drug release kinetics of bile acid-phospholipid derived liposomes;

Figure 2: Liposome formation and characterization: A-C) TEM images of neat LCA-PC (**A**), DCA-PC (**B**), and CA-PC (**C**) liposomes; **D-F**) Representative dynamic light scattering graphs of BPC liposomes developed from BPC:EggPC:DSPE-PEG using LCA-PC **(D)**, DCA-PC **(E)**, and CA-PC **(F); G-I)** Average hydrodynamic diameter **(G)**, Polydispersity index **(H)**, and Zeta potential **(I)** of LCA-PC, DCA-PC, and CA-PC liposomes from three independent experiments.

Figure 3: Doxorubicin encapsulation and biophysical characterization: A-C) Doxorubicin encapsulation efficiency (**A**), percentage of phospholipid retained (**B**), entrapment efficiency (**C**) of BPC liposomes suggesting high entrapment efficacy of hydroxylated DCA-PC and CA-PC liposomes; **D-F**) Doxorubicin release from BPC liposomes against PBS, pH = 7.4 (**D**), PBS, pH = 5.0 (**E**), 10% FBS (**F**); and **G**) Average Higuchi release rate constants from two independent experiments with R^2 > 90% of BPC liposomes in different release media implying slow release of doxorubicin from LCA-PC liposomes; **H**) DPH-based membrane rigidity of BPC liposomes revealing hydrophobic nature of LCA-PC liposomes.

Figure 4: *In vitro* activities: *In vitro* cytotoxicity of doxorubicin entrapped BPC liposomes: LCA-PC, DCA-PC, and CA-PC against murine (4T1) (**A, B**) and human (MDA-MB-231) (**C, D**) breast cancer cell lines after 24 (**A, C**) and 48h (**B, D**).

Figure 5: *In vivo* activities: A) Change in tumor volume, **B**) body weight, and **C**) survival of 4T1 tumor bearing Balb/c mice treated with doxorubicin and doxorubicin entrapped BPC liposomes; **D-F**) Hepatic alkaline phosphatase (ALP) **(D)**; skeletal muscle lactate dehydrogenase (LDH) **(E)**; and cardiac muscle specific toxicity marker (CK-MB) **(F)** toxicity markers post 24h of treatment with doxorubicin and doxorubicin encapsulated LCA-PC liposomes in 4T1 tumor bearing mice; **G-H**) Pharmacokinetic profile (**G)** and analysis **(H**) of doxorubicin and doxorubicin entrapped LCA-PC liposomes in 4T1 tumor bearing Balb/c mice; **I-K**) Bio-distribution of doxorubicin and doxorubicin entrapped LCA-PC liposomes in different organs in 4T1 tumor bearing Balb/c mice after 1h (**I**), 5h (**J**), and 10 h (**K**) of dosing.

Figure 1

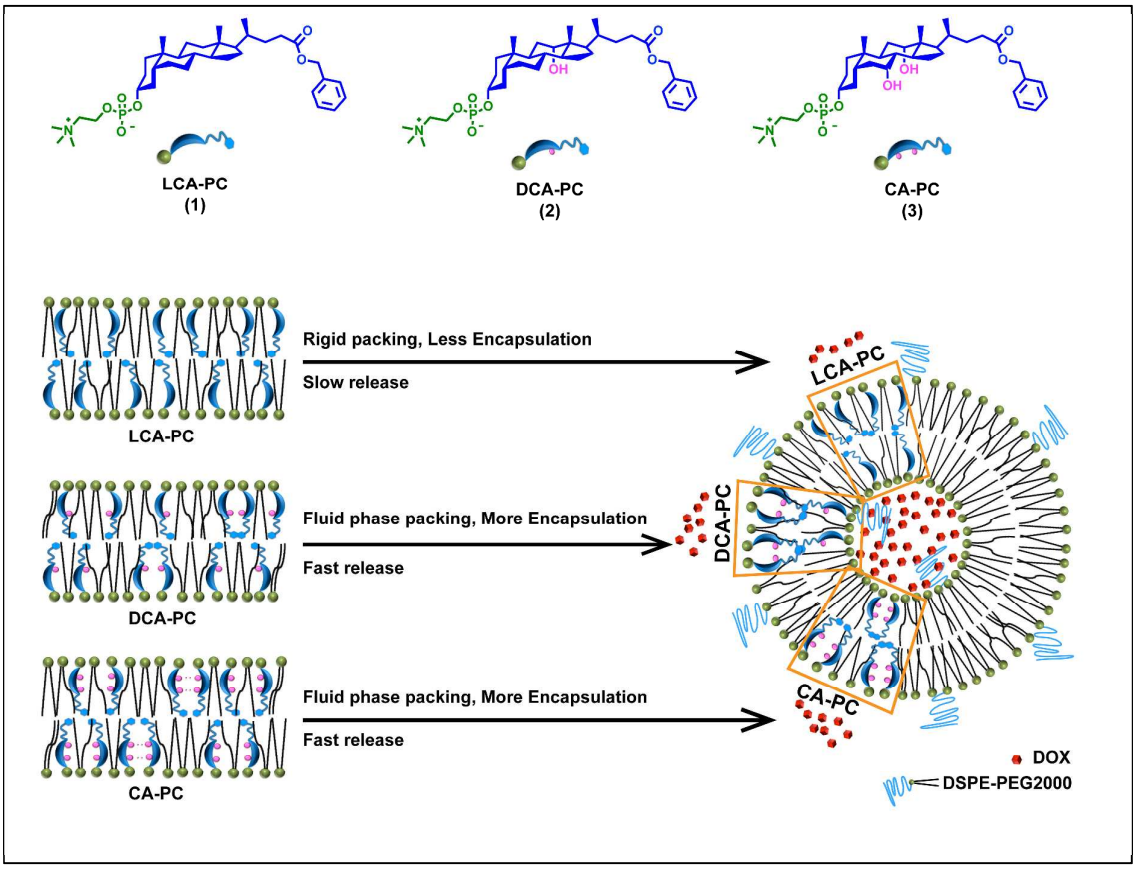
LCA-PC
(1)
DCA-PC
(2)
CA-PC
(3)
Rigid packing, Less Encapsulation
Slow release
LCA-PC
Fluid phase packing, More Encapsulation
Fast release
DCA-PC
Fluid phase packing, More Encapsulation
Fast release
CA-PC
LCA-PC
DCA-PC
CA-PC
DOX
DSPE-PEG2000

Figure 2

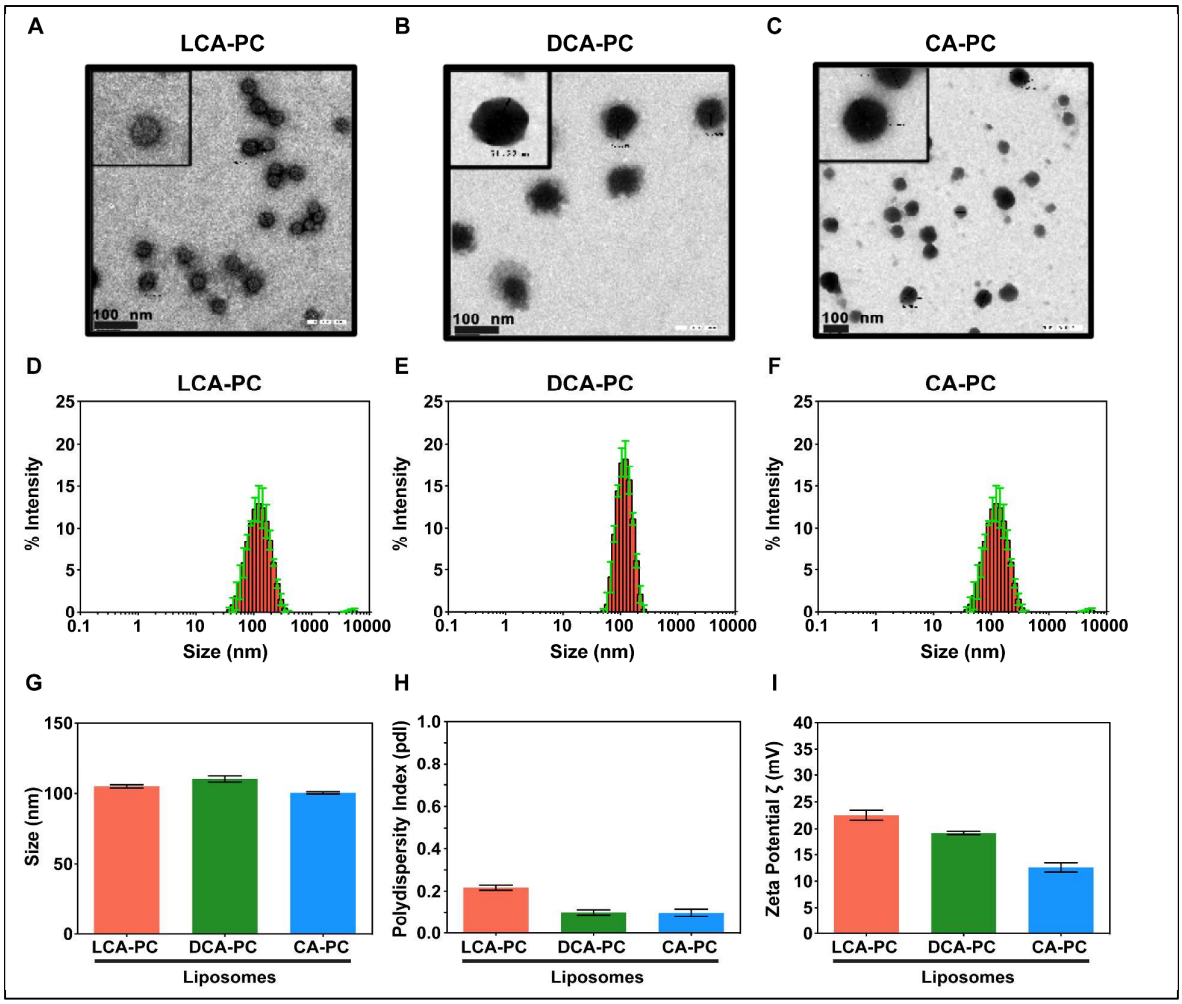
A
LCA-PC
100 nm
B
DCA-PC
100 nm
C
CA-PC
100 nm
D
LCA-PC
% Intensity
Size (nm)
E
DCA-PC
% Intensity
Size (nm)
F
CA-PC
% Intensity
Size (nm)
G
Size (nm)
LCA-PC
DCA-PC
CA-PC
Liposomes
H
Polydispersity Index (pdI)
LCA-PC
DCA-PC
CA-PC
Liposomes
I
Zeta Potential ζ (mV)
LCA-PC
DCA-PC
CA-PC
Liposomes

Figure 3

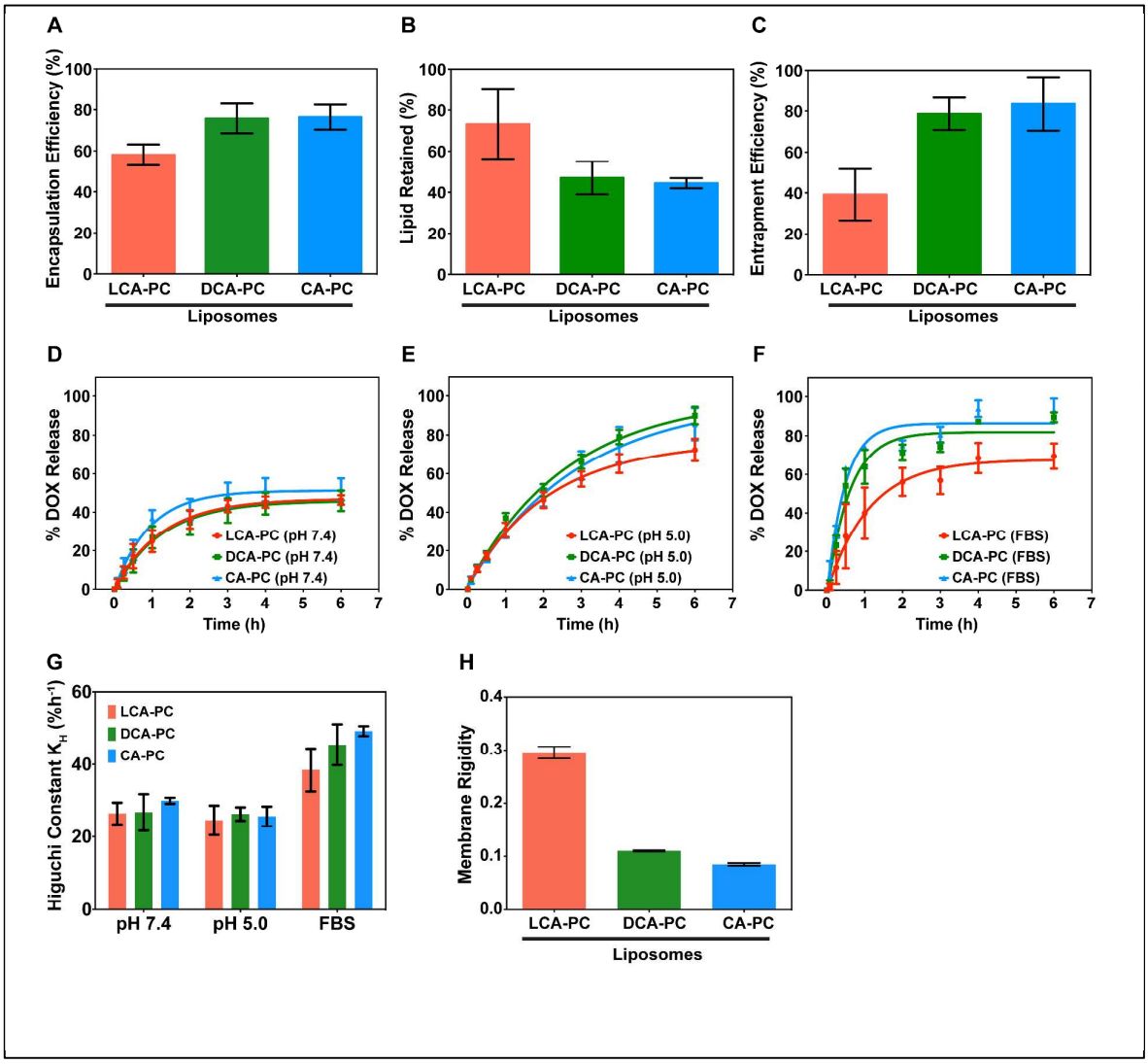
A
Encapsulation Efficiency (%)
LCA-PC
DCA-PC
CA-PC
Liposomes
B
Lipid Retained (%)
C
Entrapment Efficiency (%)
D
% DOX Release
LCA-PC (pH 7.4)
DCA-PC (pH 7.4)
CA-PC (pH 7.4)
Time (h)
E
LCA-PC (pH 5.0)
DCA-PC (pH 5.0)
CA-PC (pH 5.0)
F
LCA-PC (FBS)
DCA-PC (FBS)
CA-PC (FBS)
G
Higuchi Constant K_H (%h^{-1})
pH 7.4
pH 5.0
FBS
H
Membrane Rigidity

Figure 4

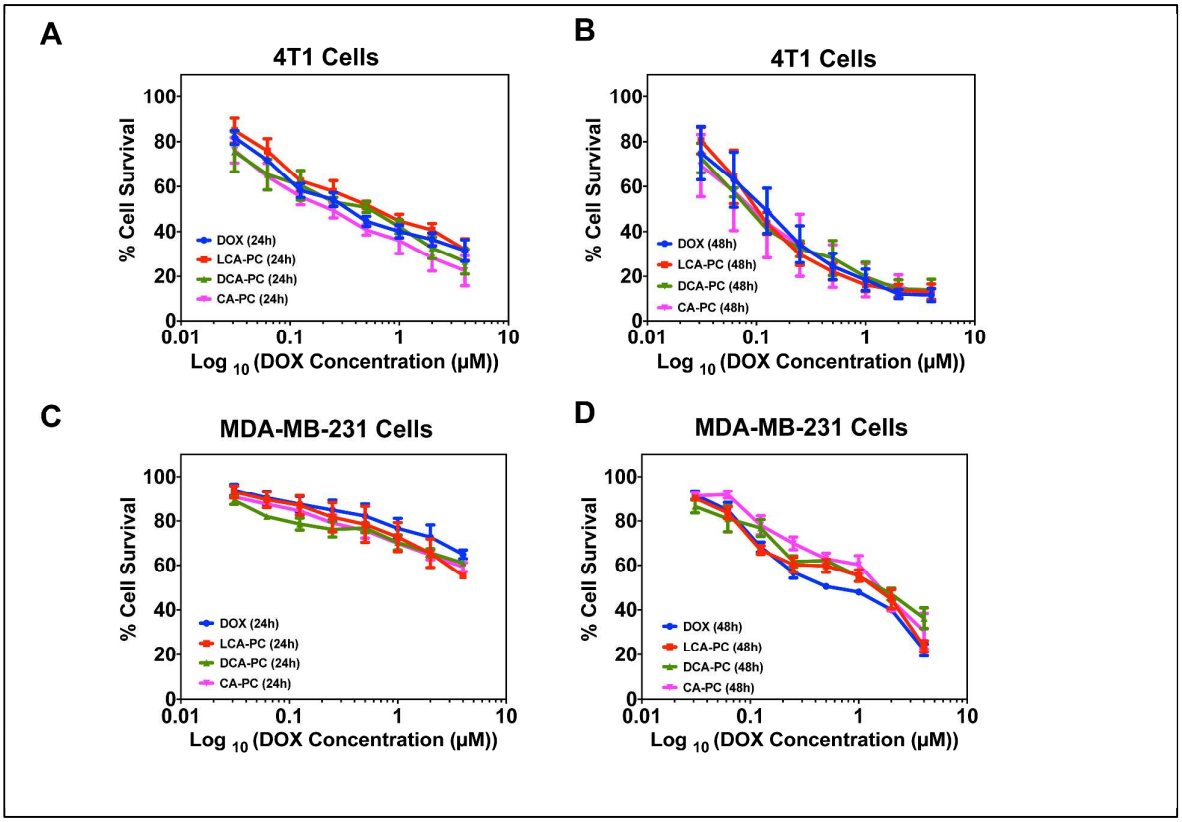
A
4T1 Cells
% Cell Survival
DOX (24h)
LCA-PC (24h)
DCA-PC (24h)
CA-PC (24h)
Log 10 (DOX Concentration (μM))
B
4T1 Cells
% Cell Survival
DOX (48h)
LCA-PC (48h)
DCA-PC (48h)
CA-PC (48h)
Log 10 (DOX Concentration (μM))
C
MDA-MB-231 Cells
% Cell Survival
DOX (24h)
LCA-PC (24h)
DCA-PC (24h)
CA-PC (24h)
Log 10 (DOX Concentration (μM))
D
MDA-MB-231 Cells
% Cell Survival
DOX (48h)
LCA-PC (48h)
DCA-PC (48h)
CA-PC (48h)
Log 10 (DOX Concentration (μM))

Figure 5

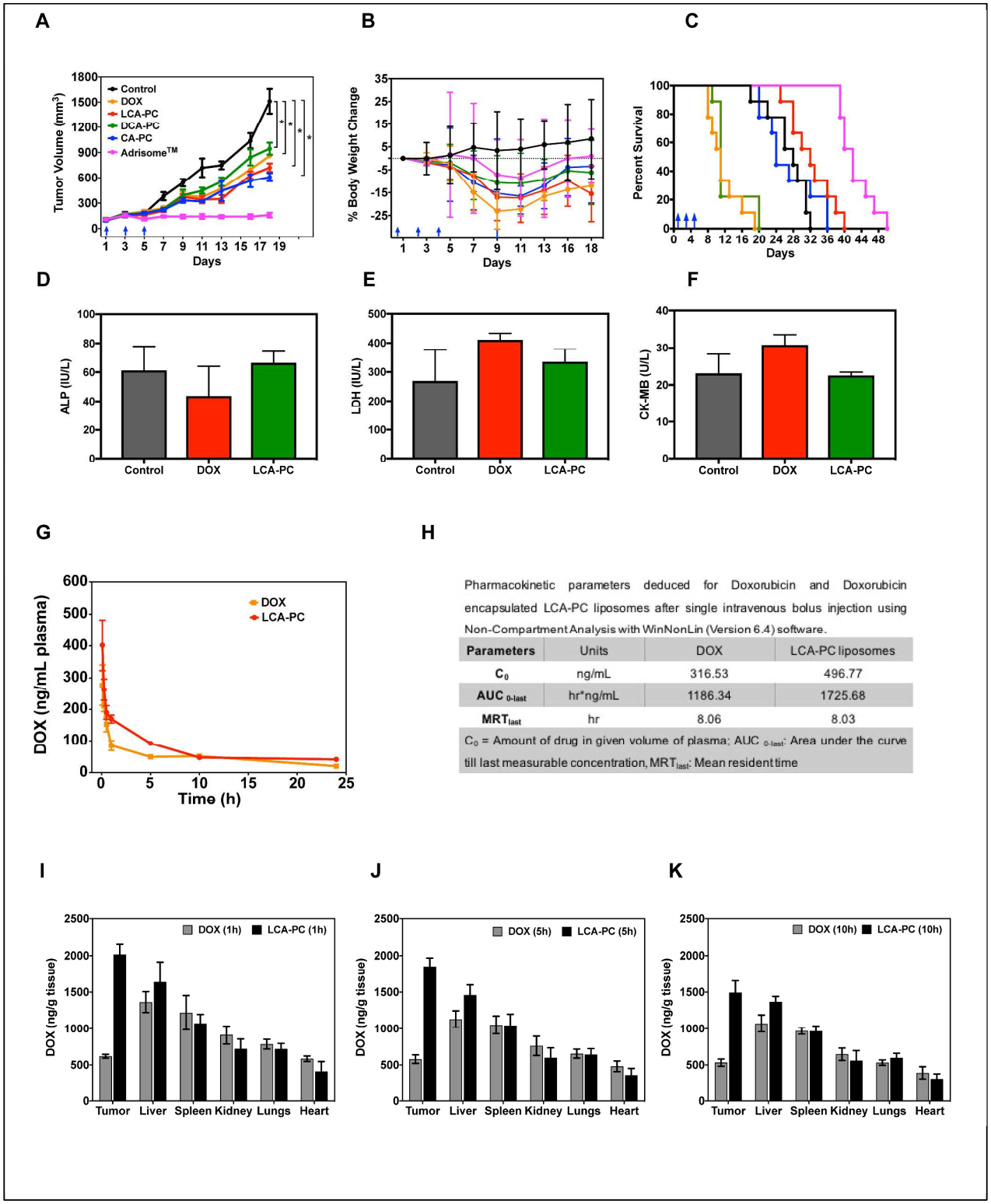

Pharmacokinetic parameters deduced for Doxorubicin and Doxorubicin encapsulated LCA-PC liposomes after single intravenous bolus injection using Non-Compartment Analysis with WinNonLin (Version 6.4) software.

Parameters	Units	DOX	LCA-PC liposomes
C_0	ng/mL	316.53	496.77
$AUC_{0\text{-last}}$	hr*ng/mL	1186.34	1725.68
MRT_{last}	hr	8.06	8.03

C_0 = Amount of drug in given volume of plasma; $AUC_{0\text{-last}}$: Area under the curve till last measurable concentration, MRT_{last}: Mean resident time

Scheme 1[a]

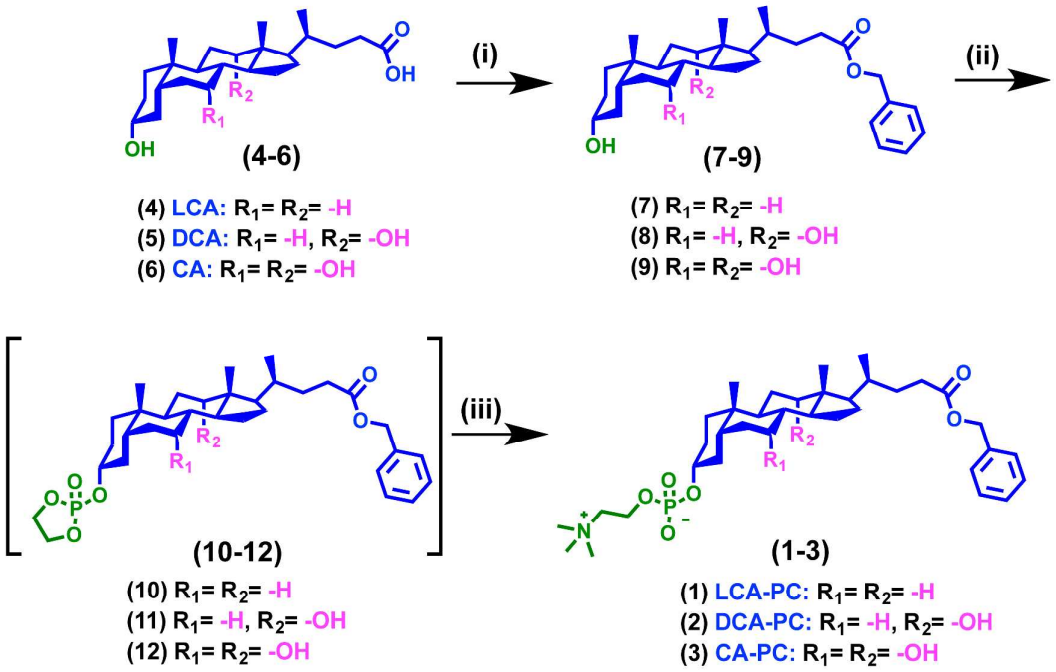

[a] **Reagents, reaction conditions, and yields:** (i) BnBr, DBU, DMF, RT, 12h, 83-88%; (ii) 2-Chloro-1, 3, 2-dioxaphospholane-2-oxide, triethylamine, 0 ˚C to RT, 8h; (iii) trimethylamine gas, acetronitrile, reflux, 24h, 60-65%.

Table of Contents